AIMS Energy

AIMS Energy, 12(5): 924–945.
DOI: 10.3934/energy.2024043
Received: 29 March 2024
Revised: 15 July 2024
Accepted: 05 August 2024
Published: 12 August 2024

https://www.aimspress.com/journal/energy

Research article

The impact of different compression ratios on emissions, and combustion characteristics of a biodiesel engine

Hussein A. Mahmood[1,*], Ali O. Al-Sulttani[2], Hayder A. Alrazen[3] and Osam H. Attia[1]

[1] Department of Reconstruction and Projects, University of Baghdad, Baghdad, Iraq
[2] Department of Water Resources Engineering, College of Engineering, University of Baghdad, Baghdad, Iraq
[3] School of Mechanical and Mining Engineering, University of Queensland, QLD, 4072, Australia

* **Correspondence:** Email: husseinadel@uobaghdad.edu.iq; Tel: +9647739695778.

Abstract: The current work investigated the combustion efficiency of biodiesel engines under diverse ratios of compression (15.5, 16.5, 17.5, and 18.5) and different biodiesel fuels produced from apricot oil, papaya oil, sunflower oil, and tomato seed oil. The combustion process of the biodiesel fuel inside the engine was simulated utilizing ANSYS Fluent v16 (CFD). On AV1 diesel engines (Kirloskar), numerical simulations were conducted at 1500 rpm. The outcomes of the simulation demonstrated that increasing the compression ratio (CR) led to increased peak temperature and pressures in the combustion chamber, as well as elevated levels of CO_2 and NO mass fractions and decreased CO emission values under the same biodiesel fuel type. Additionally, the findings revealed that the highest cylinder temperature was 1007.32 K and the highest cylinder pressure was 7.3 MPa, achieved by biodiesel derived from apricot oil at an 18.5% compression ratio. Meanwhile, the highest NO and CO_2 mass fraction values were 0.000257524 and 0.040167679, respectively, obtained from biodiesel derived from papaya oil at an 18.5% compression ratio. This study explained that the apricot oil biodiesel engine had the highest combustion efficiency with high emissions at a compression ratio of 18:5. On the other hand, tomato seed oil biodiesel engines had low combustion performance and low emissions of NO and CO_2 at a compression ratio of 15:5. The current study concluded that apricot oil biodiesel may be a suitable alternative to diesel fuel operated at a CR of 18:1.

Keywords: biodiesel; CFD; diesel engine; compression ratio

Nomenclature: B: Blend; C: Celsius; CA: Crank angle; CFD: Computational fluid dynamics; CO_2: Carbon dioxide; CO: Carbon monoxide; CR: Compression ratio; e: Rate of dissipation of turbulent kinetic energy; HC: Hydrocarbon emissions; K: Kelvin; k: turbulent kinetic energy; NO: Nitric oxide; NOx: Emissions of nitrogen oxides; P: Pressure; Pa: Pascal; PISO: Pressure-velocity calculation procedure for the Navier-Stokes equations; PM: Particulate matter; RANS: Reynolds averaged Navier Stokes; RNG: Renormalization group; TAB breakup: Taylor analogy breakup; T: Temperature

1. Introduction

Energy is an essential factor in the persistence of human life on Earth. Countries' energy consumption influences aspects such as expanding populations, resources for energy, environmental circumstances, political changes, growth rate, and implemented economic strategies [1]. Energy is employed in numerous fields, such as manufacturing, the production of food, the agricultural sector, and transportation. Rising consumption of energy and environmental problems, especially the effect of global warming, need the adoption of substitutes for fossil fuels [2]. Diesel engines are extensively implemented in many different applications, including manufacturing, agriculture, construction, and transportation, due to their enhanced fuel economy, robustness, dependability, and distinct power production [3]. Nonetheless, diesel engines are well-recognized to be the primary sources of emissions of nitrogen oxides (NOx) and particulate matter (PM) [4]. Because of decreased oil reserves, growing environmental consciousness, and tight emission restrictions, scientists are looking for clean, alternative, renewable energy sources to improve the efficiency of internal combustion engines and reduce emissions [5].

Biodiesel is regarded as one of the best substitutes for diesel fuel because of its renewable nature, low emissions, excellent combustion efficiency, biodegradability, and enhanced lubrication [6]. Biodiesel may be produced from natural resources such as fats from animals and plants. Biodiesel is an ecologically friendly fuel that is non-toxic and biodegradable in the natural environment [7]. On the other side, biodiesel fuel has cleaner combustion, a higher flash point, improved engine performance, and no sulfur concentration compared to diesel fuel [8,9]. Studies on biodiesel fuels have recently increased, and scientists think that biodiesel produced from a range of materials could be employed as a suitable alternative for traditional diesel fuel [10]. The utilization of biodiesel at various rates of diesel fuel in diesel engines involves different impacts on engine efficiency and emission levels based on the conditions of operation, engine structure, and biodiesel fuel properties [11]. Overall, biodiesel fuels have a lower thermal value than diesel fuel, although biodiesel fuels have a higher density. Several studies indicate that utilizing biodiesel derived from different feedstocks can improve emission attributes while reducing performance slightly [12].

Numerous investigations have been accomplished to enhance diesel engine efficiency and eliminate emissions in a variety of ways, such as employing biodiesel as a substitute to diesel fuel, mixing diesel fuel with various ratios of biodiesel, changing engine compression percentages, improving the chamber of the engine's combustion, and adding nano components [13]. The compression ratio is one of the most important factors for an engine. The compression ratio of a diesel engine has an important effect on its efficiency and overall performance, and it plays a crucial role in determining its efficiency, power output, fuel economy, emissions, and overall performance [14]. Various studies have been carried out to examine the impact of compression percentages on blends of biodiesel and diesel. Renish et al. [14] checked the impact of a diesel engine under various compression proportions operating with a sea mango biodiesel-diesel blend (B20). According to the results, at CR 18:1, the levels of smoke, hydrocarbons, and carbon monoxide emissions under B20 were 26.78%, 23.44%, and 37.76%, respectively, which is lesser than those of diesel. Nonetheless, the results discovered that the blend (B20) emitted more NO at every compression ratio. In addition, the effects of combustion gas recirculation rates and compression proportions of 18:1, 20:1, and 22:1 on diesel engines that were powered by a B20 blend consisting of mango seed methyl ester and diesel were investigated by Ahamed et al. [15]. The results explained that at a compression proportion of 22:1, the thermal efficiency of the brakes increased by 7.4%, while emission levels of hydrocarbons, smoke, and carbon monoxide decreased by 40%, 7.1%, and 33.3%, correspondingly. In addition, the NOx emissions climbed considerably. Datta et al. [16] studied the influence of employing a mixture consisting of biodiesel derived from palm oil with diesel as fuel under various compression proportions on efficiency of combustion and pollutants of the diesel engine. The results showed that a decline in compression proportion raises emissions ratios of smoke, hydrocarbons, and carbon monoxide but reduces emissions ratios of NOx and CO_2. Furthermore, the influence of different compression ratios inside the diesel engine that used a mixture consisting of 80% diesel fuel and 20% biodiesel made from palm oil was studied by Rosha et al. [17]. The outcomes demonstrated that increasing the engine compression ratio from 16:1 to 18:1 raised the maximum pressure inside the cylinder and the efficiency of the brake thermal, while lowering the duration of ignition delay. Moreover, as the engine's compression proportion raised from 16:1 to 18:1, emissions levels of smoke, hydrocarbons, and carbon monoxide decreased, but emissions ratios of nitrogen oxides raised. Sivaramakrishnan et al. [18] examined the properties of a diesel engine operated with mixtures of biodiesel created from karanja oil and diesel fuel under various compression ratios. The outcome showed that CO and HC emissions dropped as the blend ratio increased. Dugala et al. [19] studied the characteristics of a dual biodiesel blend of mahua and jatropha in equal proportions with diesel under various compression percentages. The results demonstrated that the highest temperature and pressure of the mixture inside the combustion chamber were 11.1–69.8 C and 0.15–0.36 bar, respectively. Moreover, the results stated that emission levels of HC and CO were decreased by 33–62%. Mahmood et al. [20] examined the impact of altering the compression proportion on the efficiency and emission properties of a diesel engine fueled by a blend of biodiesel derived from corn oil and standard diesel fuel. The results indicated that when the compression percentage and ratio of the biodiesel mixture increased, emission levels of carbon monoxide, hydrocarbons, and smoke opacity dropped. However, the emissions of carbon dioxide and nitrogen oxides raised.

Various investigations have been conducted to improve the economy of fuel and reduce pollution during the transformation of a diesel engine to run on a biodiesel-diesel blend. Several studies have looked at the influence of compression proportions on a biodiesel-diesel blend, but only a few studies have focused on pure biodiesel types derived from apricot oil, papaya oil, sunflower oil, and tomato seed oil. As a result, essential research on the optimization of the compression ratio, combustion characteristics, and pollution for a diesel engine operating with biodiesel derived from apricot oil, papaya oil, sunflower oil, and tomato seed oil is still limited. In general, the engine's efficiency and emissions depend on the temperature and pressure inside the engine, which are directly related to the air-fuel ratio, compression ratio, injection time, ignition time, and the carbon, oxygen, and hydrogen content in the fuel. The carbon, oxygen, and hydrogen content of each type of biodiesel differs from the others depending on the source from which it is derived. The goal of the current study is to investigate numerically the influence of varying compression percentages (15.5, 16.5, 17.5, and 18.5) on the emissions percentages and the characteristics of combustion in a diesel engine with one cylinder using various types of biodiesel fuels derived from oil (apricot, papaya, sunflower, and tomato seed) as a replacement for diesel fuel. The combustion chamber model was numerically examined employing the FLUENT program.

2. Computational modeling

A computational fluid dynamics (CFD) simulation was conducted on diesel engines employing different biodiesel fuels to analyze combustion properties at varying compression ratios. The ANSYS Workbench 2016 program was utilized for creating the geometry of the combustion chamber and grid generation [21]. This investigation involved a running diesel engine with a single-cylinder, a hemispherical bowl-shaped piston, a direct injection, and a four-stroke cycle using biodiesel fuel at 1500 rpm. Apricot oil, papaya oil, sunflower oil, and tomato seed oil were used to produce biodiesel fuels. Tables 1 and 2 present the specifications of the diesel engine and the characteristics of the biodiesel fuel. The FLUENT program version 16 was employed to model the combustion within an engine by addressing the governing equations linked to combustion and analyzing the outcomes. The Reynolds averaged Navier Stokes equations (RANS) are the fundamental equations of computational fluid dynamics (CFD). In addition, the three dimensions pressure-based implicit unsteady solver was employed to resolve the primary governing equations, which included momentum, mass, energy, and species. ANSYS FLUENT relies on the pressure adjustment methodology and implements the PISO approach. At the same time, the influence of turbulence on the flow was simulated using the RNG k-e model [22]. During the fuel spraying process, both the collision and TAB breakup models were employed [23]. To resolve the equation of species, discrete phase injection was coupled with finite rate/eddy dissipation chemical reactions and the equation of species transport [24]. As seen in Figure 2, just a 30° sector of the combustion chamber's geometry was determined in order to minimize the computation required. The in-cylinder geometry was created using the ANSYS tool design modeler, which started with a closed intake valve and ended with an open exhaust valve. The exhaust port, the intake port, the exhaust valve, and the intake valve were all disregarded. In addition, the complete modeling procedures, including the stroke of compression, injection of fuel, procedures of combustion, and stroke power, were simulated. The simulation process began at a 320-degree crank angle (CA) and concluded at a 400-degree CA, including both compression and combustion phases. The utilized boundary conditions were as follows: the beginning pressure was 1.57 bar, and the starting temperature was 600 K. Furthermore, the Harden burg auto-ignition model was employed to calculate the complicated chemical kinetics [25,26]. The amount of fuel injected into the engine was 0.000614727 kg/s, 0.000610534 kg/s, 0.000616971 kg/s, and 0.000618828 kg/s for sunflower oil, tomato seed oil, papaya oil, and apricot oil, respectively. ANSYS Workbench software was used for modeling biodiesel combustion. The biodiesel reaction included global sequences of reactions defined by the following equations [27].

$$C_{17}H_{33}O_2 + 24.25\,(O_2) \rightarrow 17\,CO_2 + 16.5\,H_2O + \text{Heat} \tag{1}$$

$$C_{17}H_{31}O_2 + 23.75\,(O_2) \rightarrow 17\,CO_2 + 15.5\,H_2O + \text{Heat} \tag{2}$$

$$C_{18}H_{33}O_2 + 25.25\,(O_2) \rightarrow 18\,CO_2 + 16.5\,H_2O + \text{Heat} \tag{3}$$

$$C_{17}H_{32}O_2 + 24\,(O_2) \rightarrow 17\,CO_2 + 16\,H_2O + \text{Heat} \tag{4}$$

$$H_2 + 0.5O_2 \leftrightarrow 2H_2O \quad (5)$$

$$CO + H_2O \leftrightarrow CO_2 + H_2 \quad (6)$$

The emissions of NOx were calculated employing the method of an expanded Zeldovich [28].

$$N_2 + O \leftrightarrow NO + N \quad (7)$$

$$N + O_2 \leftrightarrow NO + O \quad (8)$$

$$N + OH \leftrightarrow NO + H \quad (9)$$

Table 1. Diesel engine details [25].

Engine sort	direct injection diesel
Model	AV1 (Kirloskar)
Compression ratio	15.5, 16.5, 17.5, and 18.5
Swept volume (liter)	0.552
Valves number	2
Cylinder count	1
Stroke	110 mm
Bore	80 mm
Combustion chamber shape	bowl
Injector pressure	220 bar

Table 2. Properties of biodiesel [3,29,30].

Biodiesel	Sunflower oil	Tomato seed oil	Papaya oil	Apricot oil
Chemical formula	$C_{17}H_{33}O_2$	$C_{17}H_{31}O_2$	$C_{18}H_{33}O_2$	$C_{17}H_{32}O_2$
Density (kg/m^3)	881.5	883	840	855
Dynamic viscosity (Pa*s)	0.00366	0.004415	0.0029652	0.0036423
Kin. viscosity @ 40 ℃ (cSt)	4.4	5	3.53	4.26
Specific gravity (g/cm^3)	0.881	0.883	0.840	0.85
Lower calorific value, MJ/kg	39.91	36.67	38	40
Cetane number	46.7	47.7	48.29	50.45
Stoichiometric air-fuel ratio	12.375	12.46	12.33	12.293
Flash point (c)	162	190	112	105
Cloud point (c)	7.2	12	2	−7
Pour point (c)	−15	−16.1	1	−8
TAN (mg KOH/g)	0.22	0.74	0.42	0.25
Sulfur contents (%)	0.012	0.0172	0.01	0.00015
Sulfated ash (wt%)	0.01	0.02	0.02	0.0299
Oxygen content (wt%)	12.8	11.29	11.27	11.21
Carbon content (wt%)	75.3	75.41	75.9	75.23
Hydrogen content (wt%)	11.5	11.57	11.72	11.72

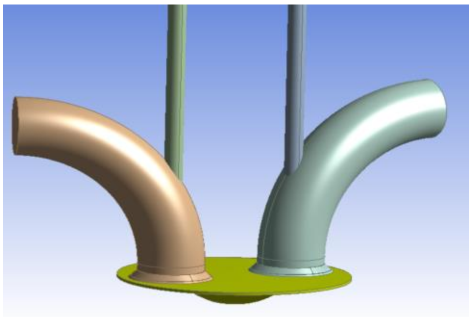

Figure 1. A depiction of the engine's cylinder geometry as generated by the ANSYS Workbench application.

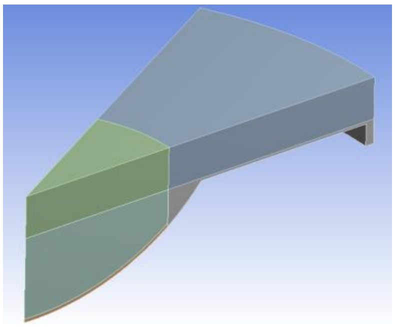

Figure 2. A demonstration of the engine's cylinder geometry through a 30-degree sector.

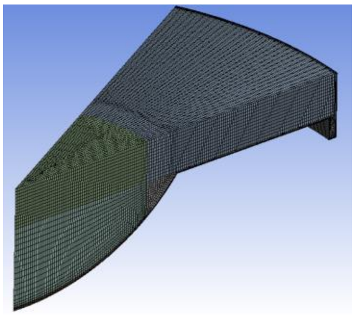

Figure 3. A display of the meshing regions of the chamber of combustion.

2.1. The examination for mesh independence

The examination for mesh independence was conducted for the combustion chamber model using a compression ratio of 15.5 and biodiesel fuel produced from apricot oil. Four different mesh sizes were created, as depicted in Table 3 and Figure 4. To demonstrate the mesh independence test, a simulation was carried out for every mesh. Figure 5 displays the calculated maximum temperature within the combustion chamber. The findings reveal that there is no noticeable variation in temperature outcomes among the four mesh sizes. According to the mesh dependence test, mesh 3 was chosen for its precise results and its minimum calculation duration.

Table 3. A display of the details of the four meshes.

Cases	Elements	Nodes
Mesh 1	50272	56062
Mesh 2	102236	111486
Mesh 3	253948	253948
Mesh 4	642033	673088

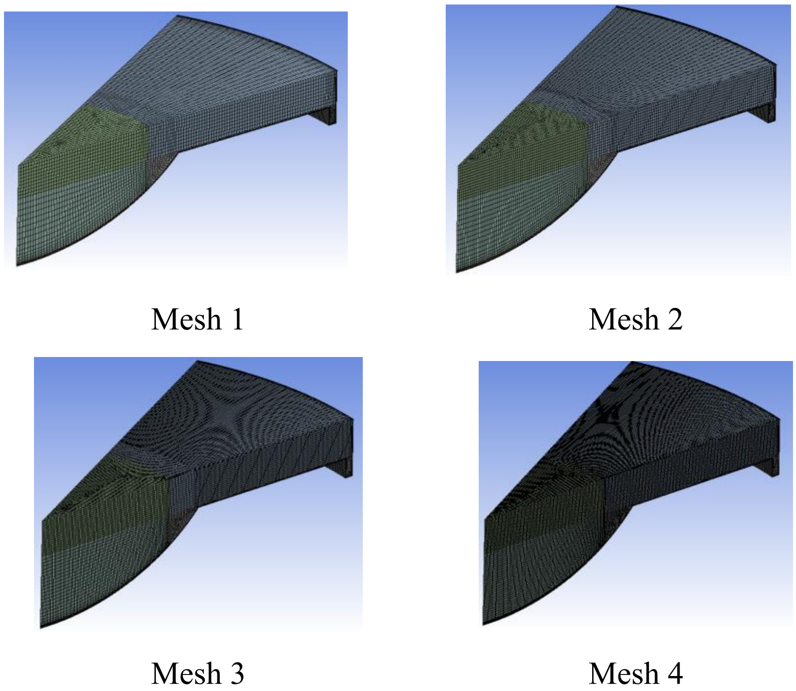

Figure 4. A display of the four meshes of varying sizes.

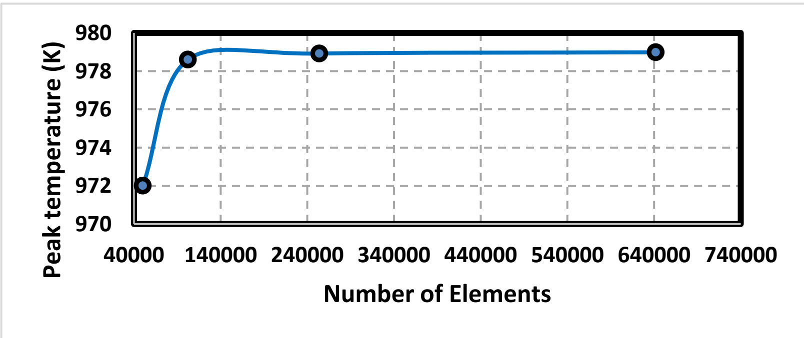

Figure 5. A display of the outcomes of the mesh independence examination.

2.2. Validations of the models

A combustion chamber model containing a single cylinder was built and tested for validation. A simulated model of a 3D engine was contrasted with Rajeesh et al.'s experimental model [23].

Comparisons were conducted at a 16.5 compression ratio, a temperature of 300 K, the engine running at 1500 rpm, and employing a mixture of fuel consisting of 80% diesel fuel and 20% chicken fat biodiesel. The pressure inside the combustion chamber obtained by computational analysis was matched with the experimental findings of Rajeesh et al. [23]. Figure 6 illustrates the combustion chamber pressure validation findings. In general, numerical analysis findings and experimental findings of Rajeesh et al. appeared to be in reasonable agreement at the majority of the points.

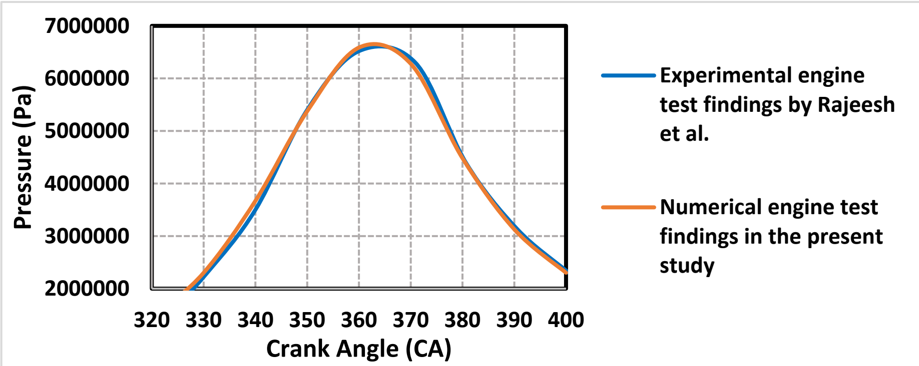

Figure 6. An illustration of the combustion chamber pressure validation findings.

3. Results

The combustion properties are significantly affected by the fuel parameters as heat is generated by combustion, concentrations of oxygen, cetane number, and the modulus of bulk. Distinct changes in biodiesel fuel characteristics are anticipated to result in a noticeable variance in combustion characteristics. Four different biodiesel fuels generated from apricot oil, papaya oil, sunflower oil, and tomato seed oil were used to study the impact of compression percentages (15.5, 16.5, 17.5, and 18.5) on the efficiency of biodiesel combustion. ANSYS Workbench 16 was used to analysis the compression ratios' impact on the combustion properties of biodiesel fuel. Below are the simulation findings for the combustion properties of biodiesel fuels under different compression ratios.

3.1. Pressure

Figure 7 illustrates the correlation between the volume-average pressure estimated within the combustion engine and the degree of crank angle under various compression ratios and different biodiesel fuels. Figure 8 shows the peak volume-average pressure values in the cylinder at different compression ratios and different biodiesel fuels. As exhibited in Figures 7 and 8, under the same biodiesel fuel type, with a rising compression ratio, the engine peak pressure rose as proven by [31]. This is due to the fact that the peak cylinder pressure increased due to the alteration in the volume of the burning chamber related to the variable compression ratio. In addition, with biodiesel created from apricot oil, the peak pressure increased from 6.36 MPa to 6.8 MPa, 7.11 MPa, and 7.30 MPa with compression ratios of 15.5, 16.5, 17.5, and 18.5, correspondingly. Moreover, with biodiesel generated from papaya oil, the value of maximum pressure was enhanced from 6.36 MPa to 6.80 MPa, 7.11 MPa, and 7.30 MPa with compression ratios of 15.5, 16.5, 17.5, and 18.5, correspondingly. Furthermore, with biodiesel fuel created from sunflower oil, the highest pressure value increased from 6.36 MPa to

6.80 MPa, 7.11 MPa, and 7.30 MPa for the corresponding compression ratios of 15.5, 16.5, 17.5, and 18.5. Moreover, with biodiesel derived from tomato seed oil, the value of the highest pressure was enhanced from 6.36 MPa to 6.81 MPa, 7.11 MPa, and 7.30 MPa with ratios of compression of 15.5, 16.5, 17.5, and 18.5, correspondingly. Compared to the different biodiesel fuels under various compression ratios, the maximum cylinder pressure was 7.3 MPa obtained by biodiesel derived from apricot oil at an 18.5 ratio compression while the minimum cylinder pressure was 6.36 MPa obtained by biodiesel fuel generated from apricot oil at a 15.5 compression ratio.

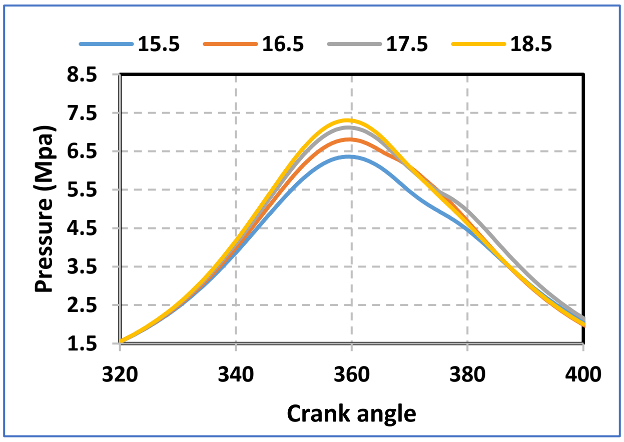

Biodiesel derived from apricot oil

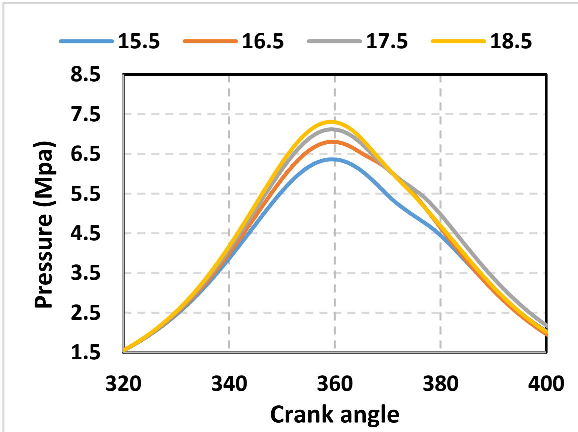

Biodiesel derived from papaya oil biodiesel

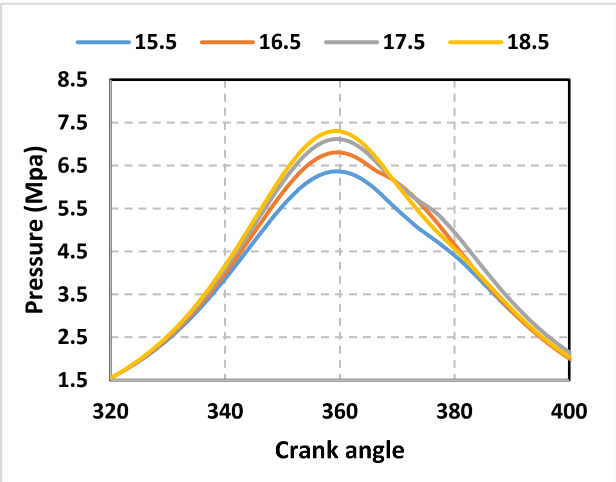

Biodiesel derived from sunflower oil

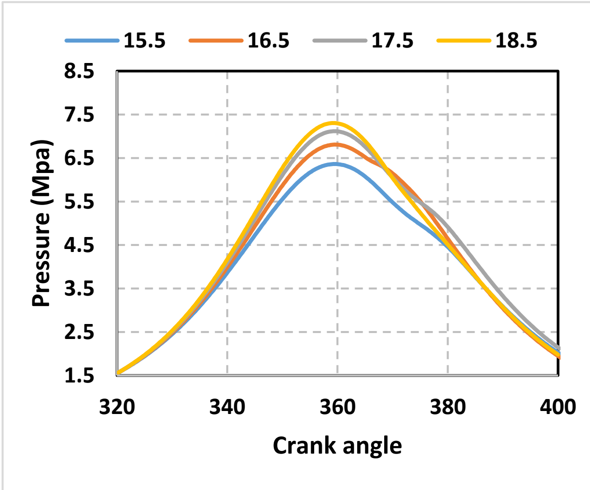

Biodiesel derived from tomato seed oil

Figure 7. The influence of compression ratios on volume-average pressure according to the crank angle under different biodiesel fuels.

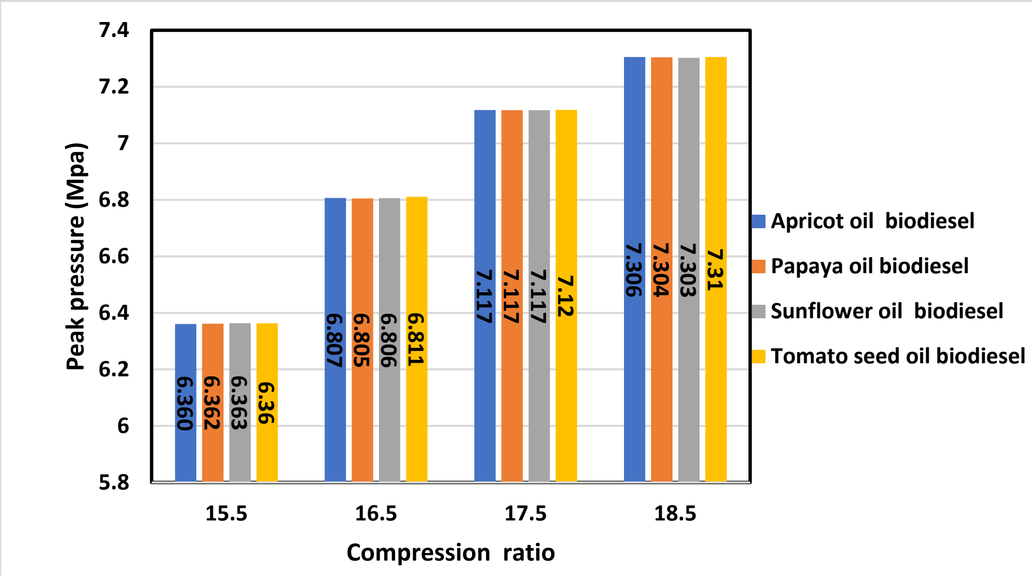

Figure 8. The maximum volume-average pressure within the combustion chamber at various compression ratios and different biodiesel fuels.

3.2. Temperature

Figure 9 displays the correlation between the volume-average temperature estimated within the combustion engine and the degree of crank angle under various compression ratios and different biodiesel fuels. Figure 10 indicates the greatest values of volume-average temperature in the engine at different compression ratios and different biodiesel fuels. As shown in Figures 9 and 10, under the same biodiesel fuel type, as compression ratios increase, the maximum temperature within the combustion chamber rises across the stroke of expansion and combustion. In addition, with biodiesel created from apricot oil, the highest temperature increased from 978.98 K to 1002.17 K, 1007.32 K, and 1064.48 K with ratios of compression of 15.5, 16.5, 17.5, and 18.5, correspondingly. Moreover, with biodiesel generated from papaya oil, the value of maximum temperature was enhanced from 991.43 K to 997.164 K, 1001.88 K, and 1055.70 K with ratios of compression of 15.5, 16.5, 17.5, and 18.5, correspondingly. In addition, with biodiesel derived from sunflower oil, the peak temperature value was improved from 992.74 K to 1001.41 K, 1003.28 K, and 1047.62 K for the corresponding compression ratios of 15.5, 16.5, 17.5, and 18.5. Moreover, with biodiesel derived from tomato seed oil, the value of the highest temperature was enhanced from 964.07 K to 992.18 K, 994.69 K, and 1052.23 K for the compression percentages of 15.5, 16.5, 17.5, and 18.5, correspondingly. In regard to the different biodiesel fuels under various compression ratios, the maximum cylinder temperature was 1064.48 K obtained by biodiesel generated from apricot oil at an 18.5 compression ratio, while the minimum cylinder temperature was 964.069 K obtained by biodiesel created from tomato seed oil at a 15.5 compression ratio. Table 4 indicates the ignition start temperature within the combustion engine and the degree of crank angle under various compression ratios and different biodiesel fuels. There are different factors that affect the ignition delay and ignition start temperature: air-fuel ratio, cetane number, engine speed, combustion chamber design, injection time and period, injection amount and pressure, engine temperature, and compression ratio. In this study, the examination was done under slightly different circumstances with the change in compression ratios.

As shown in Table 4, the ignition initiation temperature for different types of biodiesel under various compression ratios ranged between 789–832.4 K under a crank angle ranging between 365.25–370.8.

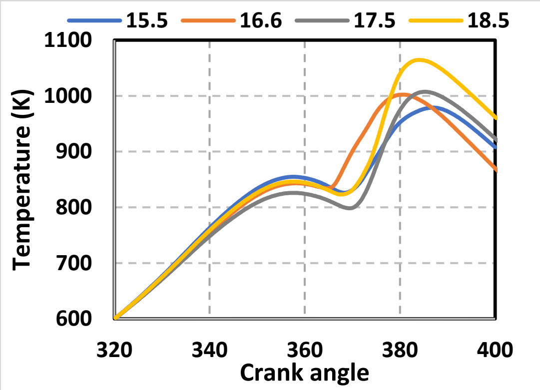	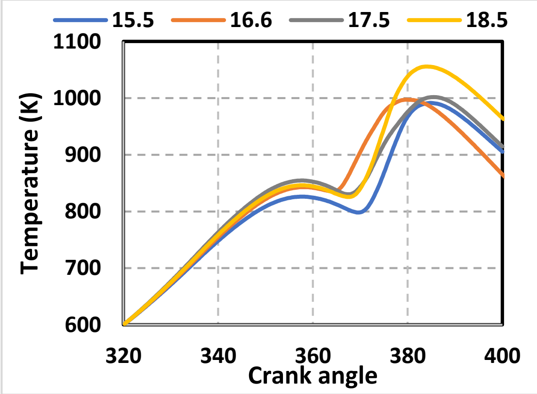
Biodiesel derived from apricot oil	Biodiesel derived from papaya oil
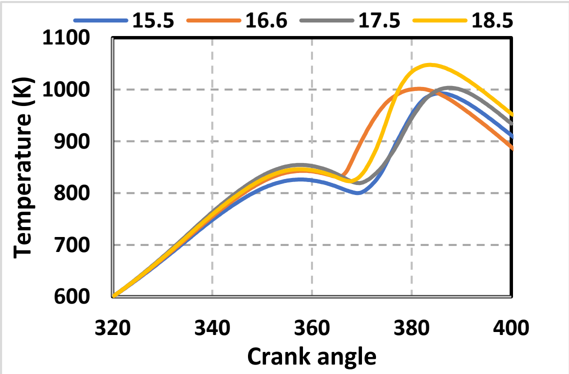	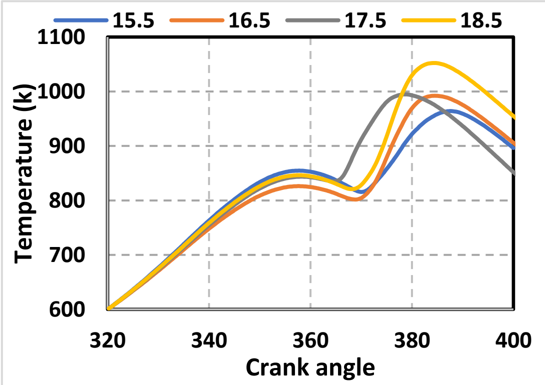
Biodiesel derived from sunflower oil	Biodiesel derived from tomato seed oil

Figure 9. The influence of the compression ratios on volume-average temperature according to the crank angle under different biodiesel fuels.

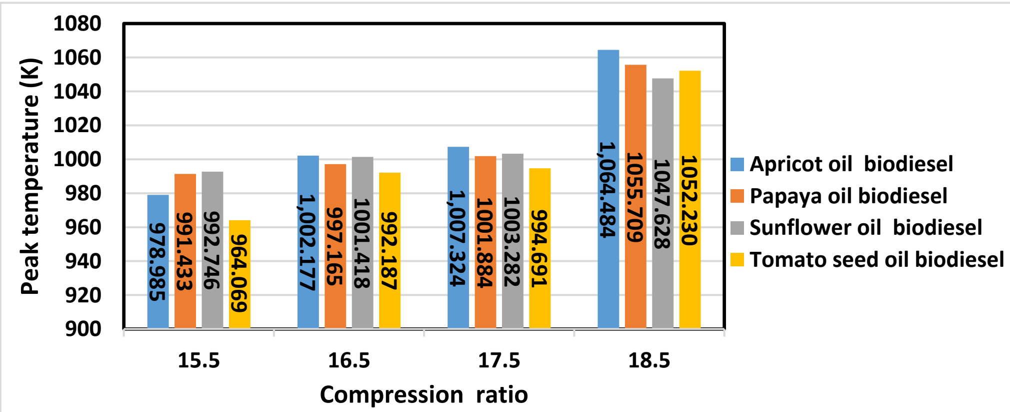

Figure 10. Highest volume-average temperature within the combustion chamber at various compression ratios and different biodiesel fuels.

Table 4. Ignition start temperatures within the combustion engine and the degree of crank angle under various compression ratios and different biodiesel fuels.

Biodiesel type	CR	Ignition start temperature (K)	Crank angle
Tomato seed oil	15.5	828.2	370.8
	16.5	801	369.5
	17.5	827.6	365.75
	18.5	821.4	368.75
Sunflower oil	15.5	800	368.75
	16.5	825.25	366.25
	17.5	829.16	369.25
	18.5	823.56	367.8
Papaya oil	15.5	798.13	369.75
	16.5	830	365.25
	17.5	832.4	369.25
	18.5	825.5	367.5
Apricot oil	15.5	829.33	369.75
	16.5	827.5	365.75
	17.5	789.47	369.75
	18.5	823.25	368.82

3.3. Carbon dioxide (CO_2)

Figure 11 exhibits the correlation between the degree of crank angle and the volume-average CO_2 emissions calculated within the engine under various compression ratios and different biodiesel fuels. Figure 12 represents the engine's highest value of volume-average CO_2 emission at different compression ratios and different biodiesel fuels. Figure 13 displays the CO_2 mass fraction formation domains on the plane inside the combustion chamber. CO_2 emissions are influenced by the process of combustion in the chamber of combustion and the oxygen concentration in the fuel. A higher concentration of CO_2 indicates that the fuel has undergone almost full combustion in the engine. Moreover, CO_2 emission is also influenced by the temperature inside the combustion chamber. Furthermore, an improved combustion process results in increased CO_2 emissions. As shown in Figures 11, 12, and 13, under the same biodiesel fuel type, as the compression ratio expands, the greatest CO_2 mass fraction value inside the combustion chamber rises, as found by [18]. In addition, with biodiesel derived from apricot oil, the CO_2 mass fraction value increased from 0.030103095 to 0.033584895, 0.03367682, and 0.038645156 for the compression percentages of 15.5, 16.5, 17.5, and 18.5, correspondingly. Moreover, with biodiesel generated from papaya oil, the value of maximum CO_2 mass fraction increased from 0.029822665 to 0.032467801, 0.03503809, and 0.040167679 for 16.5, 17.5, 15.5, and 18.5 compression ratios, respectively. In addition, with biodiesel created from sunflower oil, the peak CO_2 mass fraction value increased from 0.031532518 to 0.032430077, 0.035482766, and 0.038256764 for the compression percentages of 15.5, 16.5, 17.5, and 18.5, correspondingly. Moreover, with biodiesel from tomato seed oil, the value of the highest CO_2 mass fraction raised from 0.028922474 to 0.03256772, 0.032825675, and 0.038400801 with ratios of compression of 15.5, 16.5, 17.5, and 18.5, correspondingly. Compared to the different biodiesel fuels under various compression ratios, the maximum CO_2 mass fraction value was 0.040167679 obtained by biodiesel from papaya oil at a compression ratio of 18.5, while the minimum CO_2 mass fraction value was 0.028922474 obtained by biodiesel from tomato seed oil at a compression ratio of 15.5.

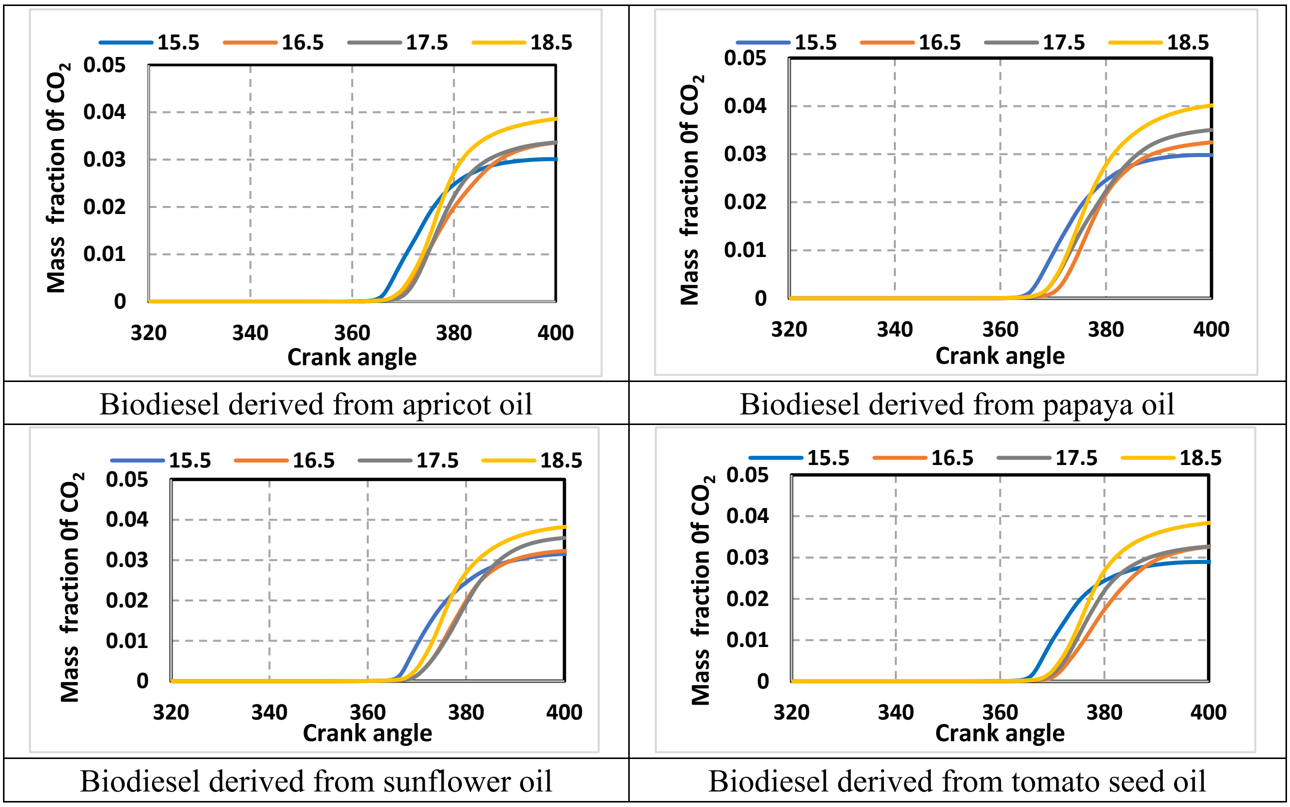

Biodiesel derived from apricot oil | Biodiesel derived from papaya oil

Biodiesel derived from sunflower oil | Biodiesel derived from tomato seed oil

Figure 11. The influence of compression ratios on volume-average CO_2 emission according to the crank angle under different biodiesel fuels.

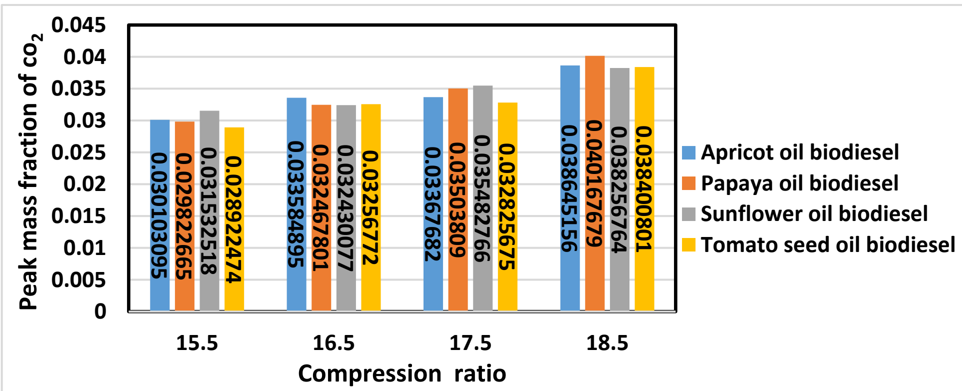

Figure 12. Highest volume-average CO_2 concentration inside the combustion chamber at different percentages of compression and different biodiesel fuels.

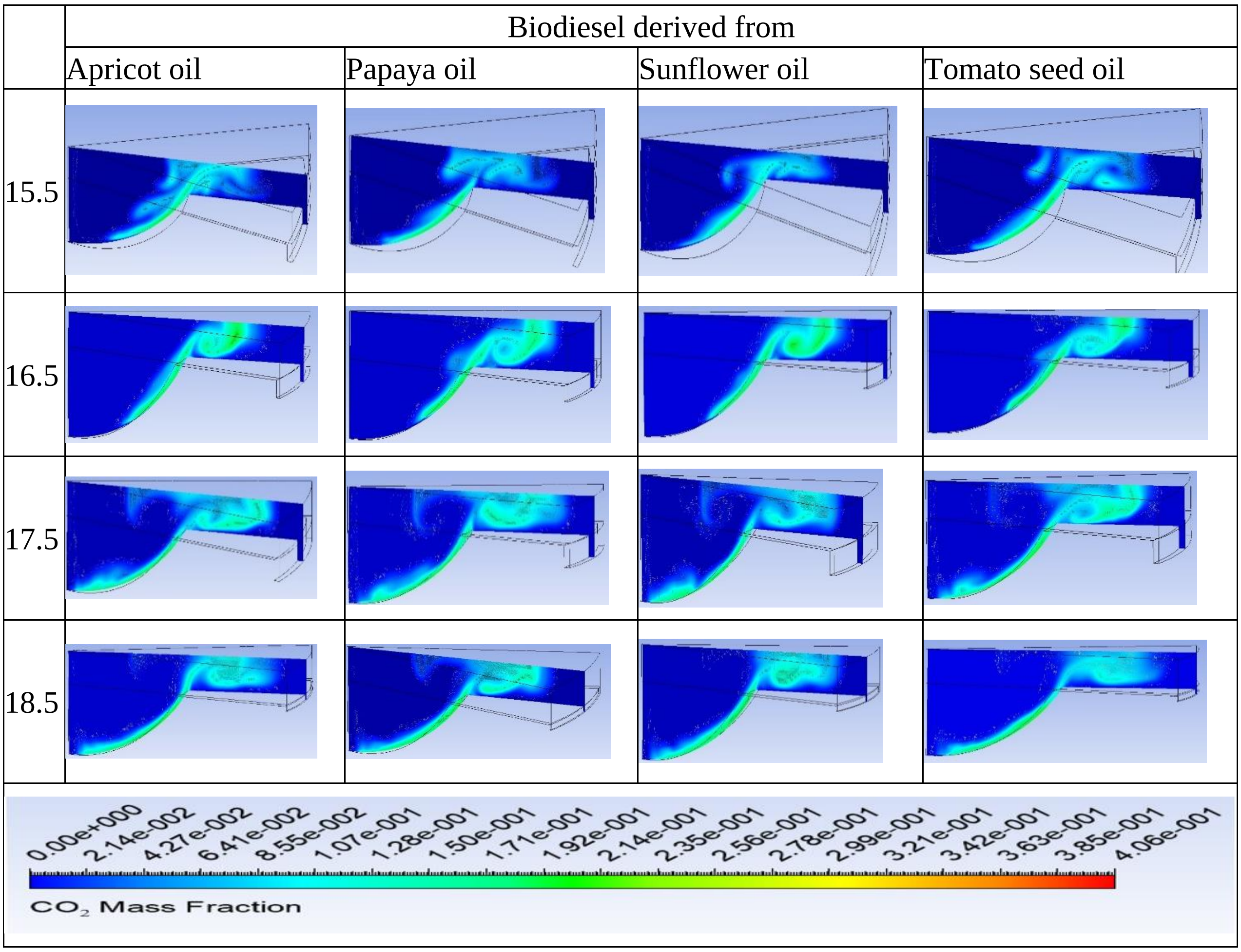

Figure 13. The spatial distribution of CO_2 emission rates.

3.4. Emission of carbon monoxide (CO)

Figure 14 presents the correlation between the volume-average CO emissions estimated within the engine and the degree of crank angle under various compression ratios and different biodiesel fuels. Figure 15 represents the engine's lowest value of volume-average CO emission at different compression ratios and different biodiesel fuels. Figure 16 displays the CO mass fraction formation domains on the plane inside the combustion chamber. CO emissions result from incomplete fuel combustion, influenced by factors such as the air-fuel percentage, oxygen deficiency, inadequate air entering to engine, mixture preparation, and insufficient combustion throughout the process of combustion. Moreover, engine characteristics such as fuel kind, ratio of equivalence, design of the cylinder, period and time of injection, speed of engine, and load influence CO emissions. As demonstrated in Figures 14, 15, and 16, under the same biodiesel fuel type, minimum CO emission values decreased with the increase of compression ratios, as found by [14]. Additionally, with biodiesel generated from apricot oil, the minimum levels of CO mass fraction in the combustion chamber declined from 2.32458E-10 to 2.08108E-10, 1.79319E-10, and 1.40973E-10 for compression ratios of 15.5, 16.5, 17.5, and 18.5, correspondingly. Moreover, with biodiesel created from papaya oil, the value of minimum CO mass fraction was enhanced from 2.21706E-10 to 1.97685E-10, 1.77581E-10, and 1.38693E-10 for the compression percentages of 15.5, 16.5, 17.5, and 18.5, correspondingly. In addition, with biodiesel derived from sunflower oil, the minimum CO mass fraction value was improved from 2.2138E-10 to 2.02897E-10, 1.8197E-10, and 1.42989E-10 with ratios of compression of 15.5, 16.5, 17.5, and 18.5, correspondingly. Moreover, with biodiesel derived from tomato seed oil, the value of the lowest CO mass fraction was enhanced from 2.18899E-10 to 2.12595E-10, 1.83351E-10, and 1.30127E-10 for the corresponding compression ratios of 15.5, 16.5, 17.5, and 18.5. As demonstrated in Figures 14 and 15, compared to the different biodiesel fuels under various compression ratios, the maximum value of the CO mass fraction at the engine outlet was 2.32458E-10 obtained by biodiesel generated from apricot oil at a compression ratio of 15.5, while the minimum value of the CO mass fraction at the engine outlet was 1.30127E-10 obtained by biodiesel created from tomato seed oil at a compression ratio of 18.5.

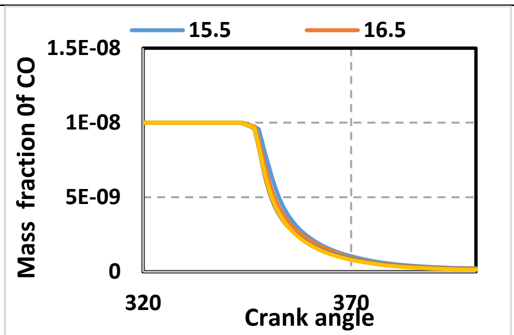

Biodiesel derived from apricot oil

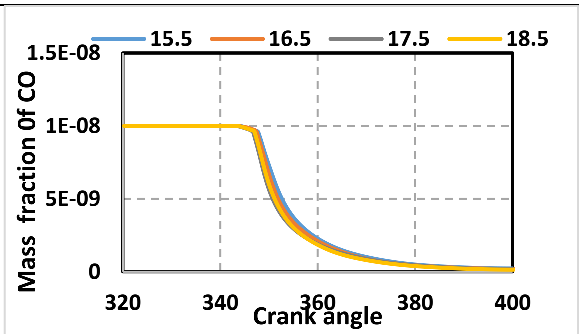

Biodiesel derived from papaya oil

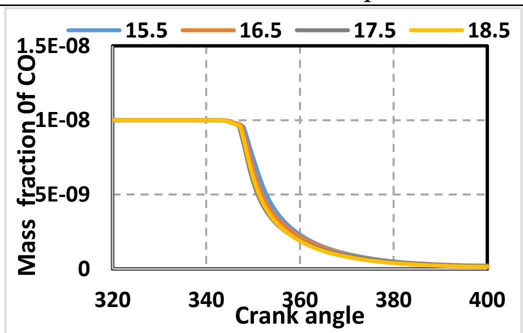

Biodiesel derived from sunflower oil

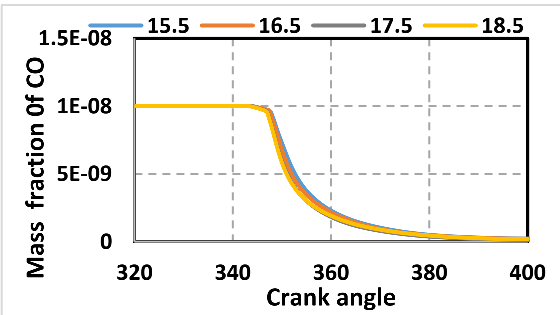

Biodiesel derived from tomato seed oil

Figure 14. The influence of compression ratios on volume-average CO emission according to the crank angle under different biodiesel fuels.

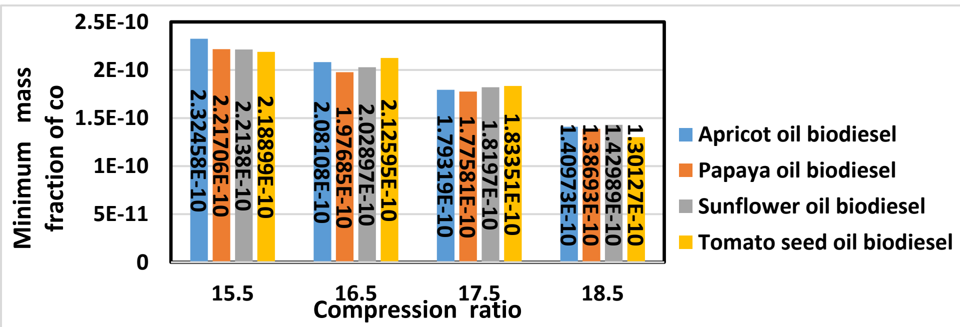

Figure 15. Highest volume-average CO concentration inside the combustion chamber at different percentages of compression and different biodiesel fuels.

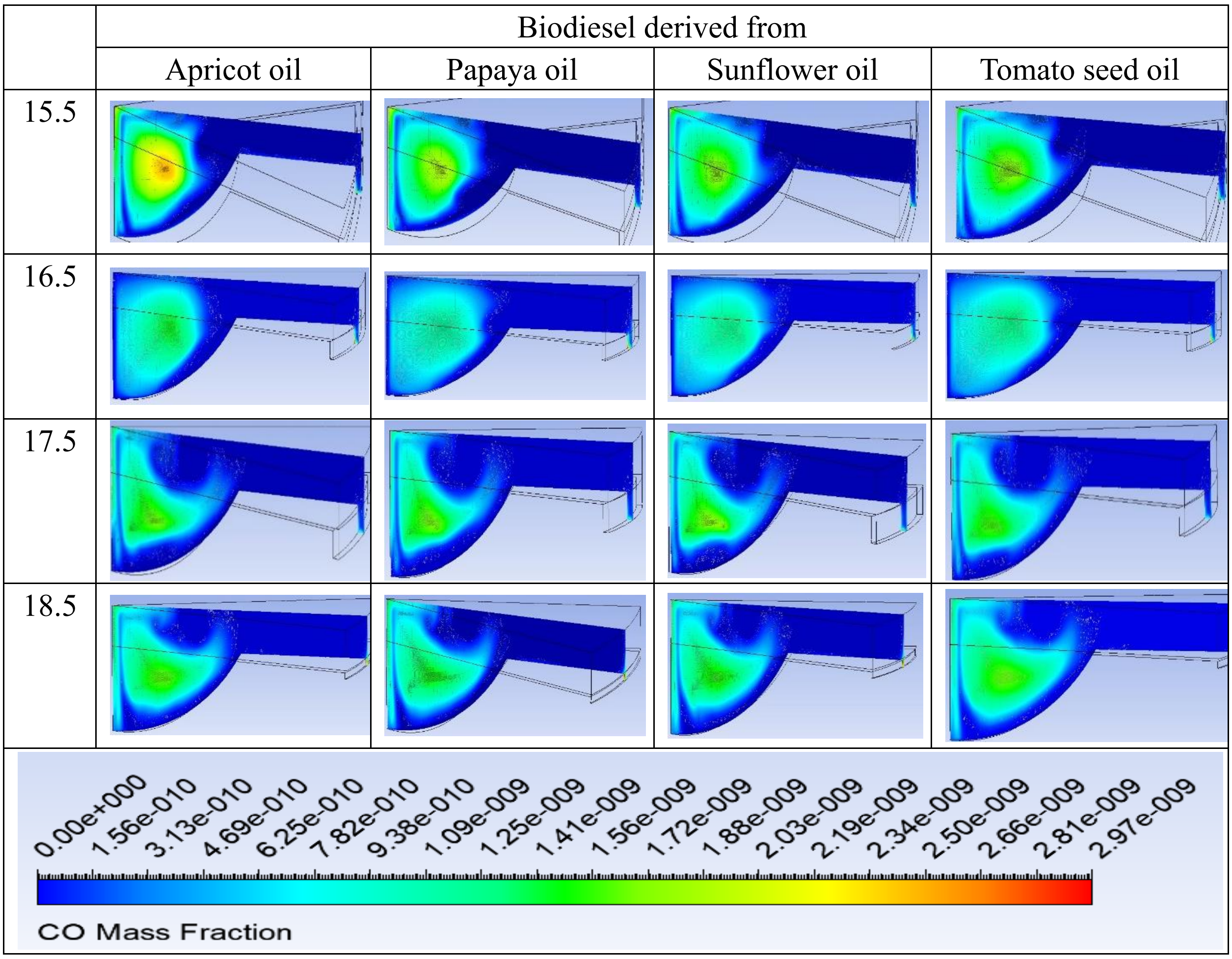

Figure 16. The spatial distribution of CO emission rates.

3.5. Emission of nitric oxide

Figure 17 displays the correlation between the calculated volume-average nitric oxide emissions inside the combustion chamber and the degree of crank angle under various compression ratios and different biodiesel fuels. Figure 18 demonstrates the peak volume-average nitric oxide emission (NO) from the engine at different compression ratios and different biodiesel fuels. Figure 19 displays the formation domains of NO mass fraction on the plane inside the combustion chamber. The amount of nitric oxide generated depends on the peak temperature inside the engine, retention duration, and oxygen content. Moreover, a lower combustion temperature reduces the NO percentage in the combustion chamber. As a result, a rise in nitric oxide emissions is significantly connected to engine temperature and oxygen concentrations. As demonstrated in Figures 7 and 8, for the same biodiesel fuel type, increasing compression ratios raises the peak NO mass fraction level inside the combustion chamber with a similar trend to [14,18]. In addition, with biodiesel from apricot oil, the NO mass fraction value increased from 0.000154334 to 0.000182226, 0.000187265, and 0.000244325 with ratios of compression of 15.5, 16.5, 17.5, and 18.5, correspondingly. Moreover, with biodiesel generated from papaya oil, the value of maximum NO mass fraction increased from 0.000149276 to 0.0001607, 0.000170888, and 0.000257524 for compression percentages of 15.5, 16.5, 17.5, and 18.5, correspondingly. In addition, with biodiesel derived from sunflower oil, the peak NO mass fraction value increased from 0.000142055 to 0.000149057, 0.000155162, and 0.000228919 for 16.5, 17.5, 15.5, and 18.5 compression ratios, respectively. Moreover, with biodiesel from tomato seed oil, the value of the highest NO mass fraction raised from 0.000122216 to 0.000156628, 0.000180591, and 0.000241274 for compression ratios of 15.5, 16.5, 17.5, and 18.5, respectively. In regard to the different biodiesel fuels under various compression ratios, the maximum NO mass fraction value was 0.000257524 obtained by biodiesel from papaya oil at an 18.5 compression ratio, while the minimum NO mass fraction value was 0.000122216 obtained by biodiesel from tomato seed oil at a 15.5 compression ratio.

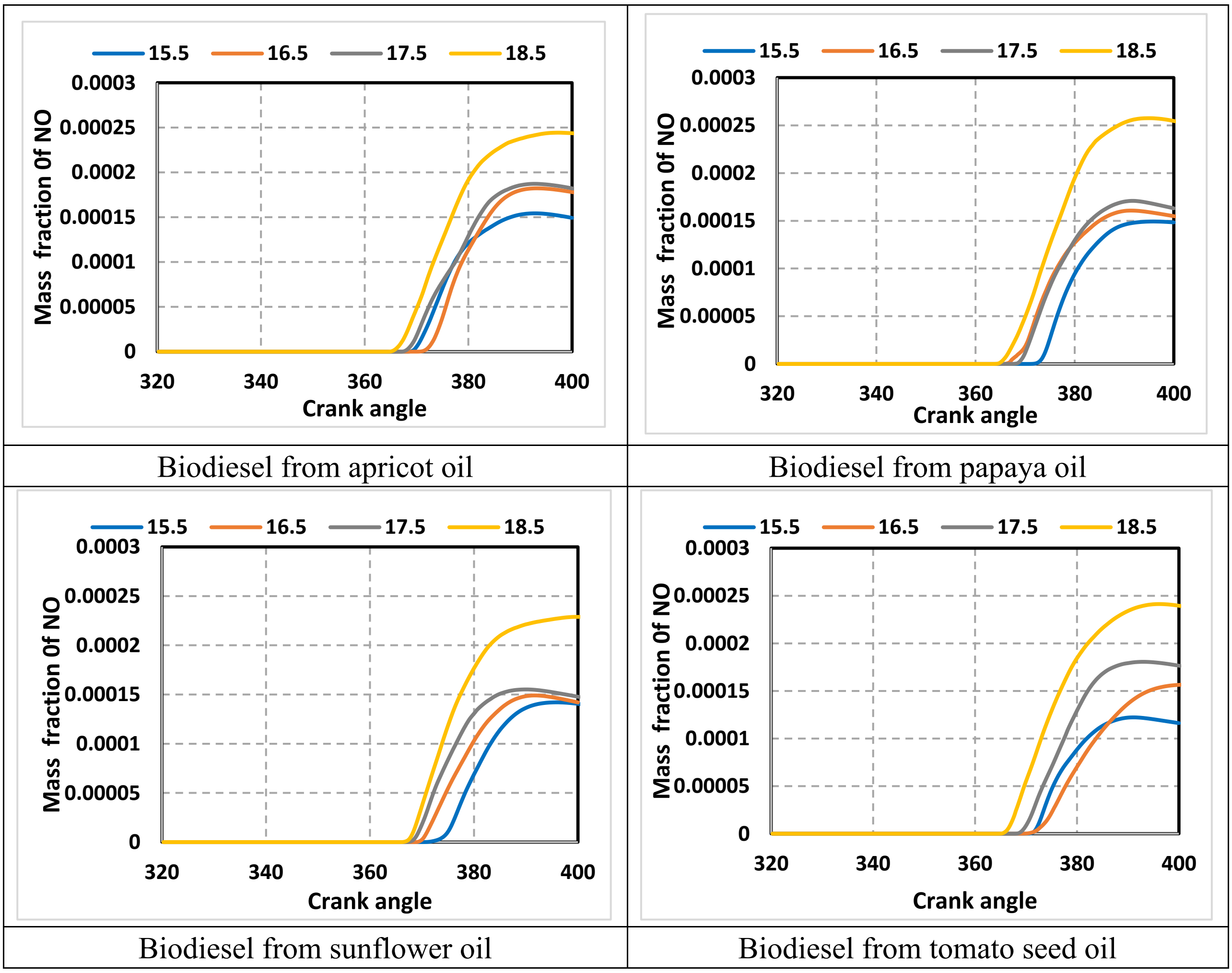

Figure 17. The influence of compression ratios on volume-average NO emission according to the crank angle under different biodiesel fuels.

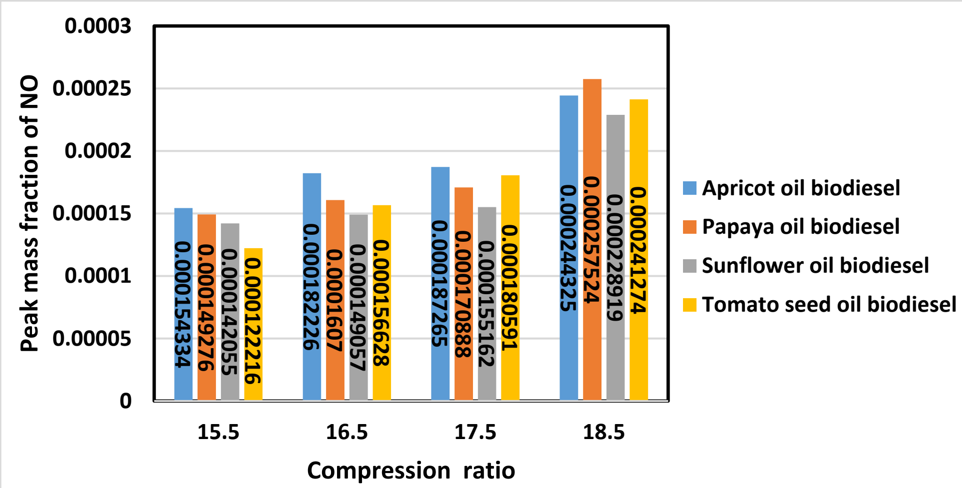

Figure 18. The highest volume-average NO concentration inside the combustion chamber at various ratios of compression and different biodiesel fuels.

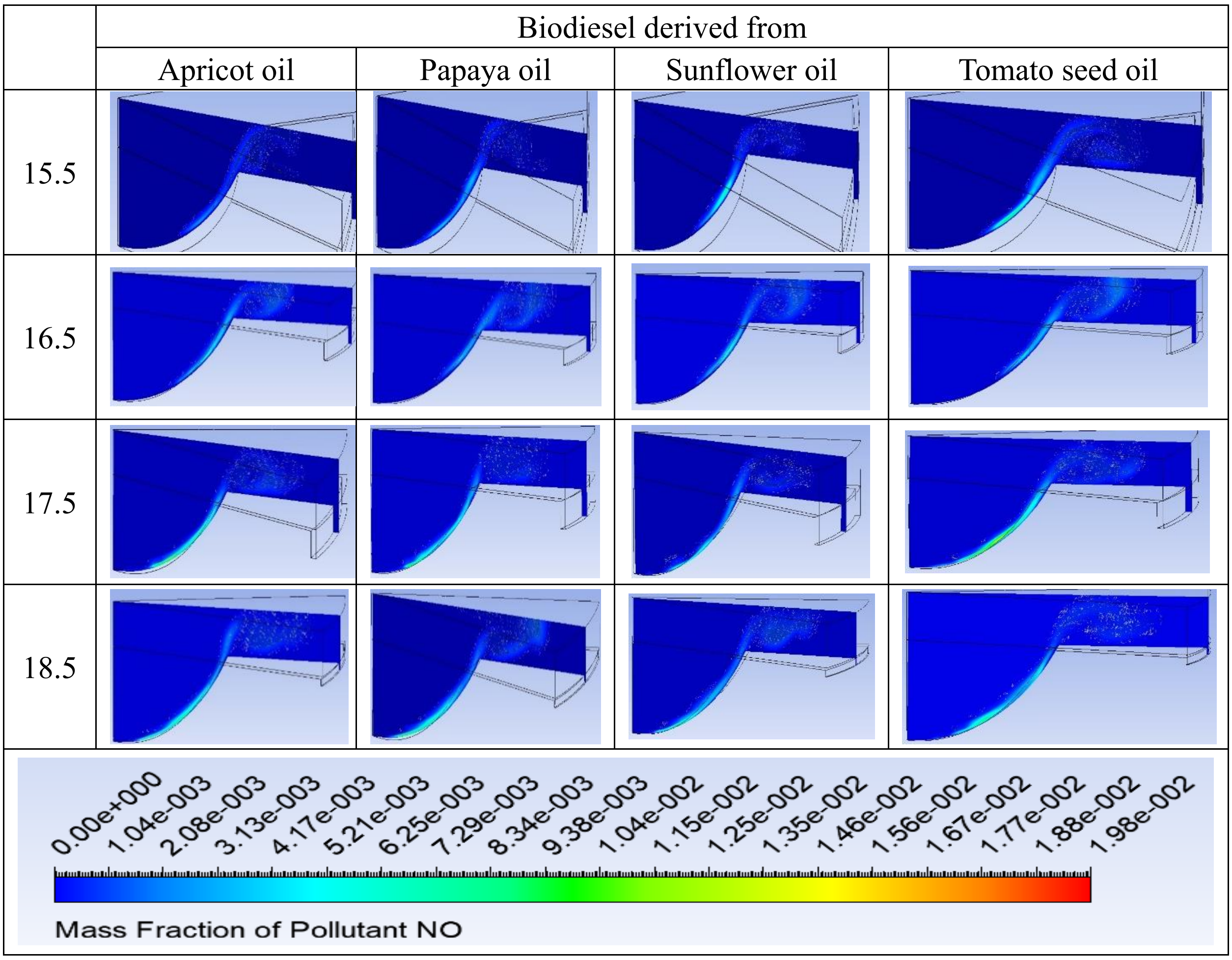

Figure 19. The spatial distribution of NO emission rates.

4. Conclusions

The current work presents the influence of varying compression ratios (15.5, 16.5, 17.5, and 18.5) on the emissions percentages and the characteristics of combustion in a diesel engine with one cylinder using various types of biodiesel fuels derived from oil (apricot, papaya, sunflower, and tomato seed) as a replacement to diesel fuel. The combustion chamber model was examined employing the FLUENT program. The study outcomes led to the following conclusions:

- Compression ratios increased under the same biodiesel fuel type. Moreover, compared to the different biodiesel fuels under various compression ratios, the maximum cylinder pressure was 7.3 MPa obtained by biodiesel from apricot oil at an 18.5 compression ratio and the maximum cylinder temperature was 1064.48 K obtained by biodiesel from apricot oil at an 18.5 compression ratio. On the other hand, the minimum cylinder pressure was 6.36 MPa obtained by biodiesel generated from apricot oil at a 15.5 compression ratio and the minimum temperature inside the engine was 964.069 K obtained by biodiesel created from tomato seed oil at a 15.5 compression ratio.
- According to numerical results, under the same biodiesel fuel type, with the increase of compression ratios, the highest CO_2 and NO mass fraction values inside the combustion chamber were raised. Moreover, compared to the different biodiesel fuels under various compression ratios, the maximum NO mass fraction value was 0.000257524 obtained by biodiesel derived from papaya oil at an 18.5 compression ratio and the maximum CO_2 mass fraction value was 0.040167679 obtained by biodiesel created from papaya oil at an 18.5 compression ratio. On the other hand, the minimum NO mass fraction value was 0.000122216 obtained by biodiesel from tomato seed oil at a 15.5 compression ratio and the minimum CO_2 mass fraction value was 0.028922474 obtained by biodiesel from tomato seed oil at a 15.5 compression ratio.
- According to numerical findings, as compression ratios increase, the minimum CO emission values decrease under the same biodiesel fuel type. Moreover, compared to the different biodiesel fuels under varying ratios of compression, the highest level of the CO mass fraction at the engine outlet was 2.32458E-10 obtained by biodiesel generated from apricot oil at a compression ratio of 15.5, while the minimum value of the CO mass fraction at the engine outlet was 1.30127E-10 obtained by biodiesel created from tomato seed oil at a compression ratio of 18.5.
- This study explained that the apricot oil biodiesel engine had the highest combustion efficiency with high emissions at a compression ratio of 18:5. On the other hand, tomato seed oil biodiesel engines had low combustion performance and low emissions of NO and CO_2 at a compression ratio of 15:5. In the current study, it can be concluded that apricot oil biodiesel may be a suitable alternative to diesel fuel operated at a CR of 18:1.

5. Future work

In future work, we will study the effects of biodiesel injection time, ignition delay, and piston shape on combustion efficiency, as well as the effects of nano materials in addition to biodiesel fuel on combustion performance.

Use of AI tools declaration

The authors declare that no artificial intelligence tools were used in this manuscript.

Acknowledgments

The authors would like to thank the University of Baghdad for their support.

Conflict of interest

The authors state that there are no conflicts of interest related to the publication of this article.

Author contributions

Hussein A. Mahmood: Writing-preparation of the original draft. Hayder A. Alrazen: Checking and verifying the simulation. Ali O.Al-Sulttani and Osam H. Attia: Review the Original draft preparation.

References

1. Mahmood HA, Al-Sulttani AO, Attia OH (2021) Simulation of syngas addition effect on emissions characteristics, combustion, and performance of the diesel engine working under dual fuel mode and lambda value of 1.6. *IOP Conference Series: Earth and Environmental Science: IOP Publishing* 779: 012116. https://doi.org/10.1088/1755-1315/779/1/012116
2. Muruganantham P, Pandiyan P, Sathyamurthy R (2021) Analysis on performance and emission characteristics of corn oil methyl ester blended with diesel and cerium oxide nanoparticle. *Case Stud Therm Eng* 26:101077. https://doi.org/10.1016/j.csite.2021.101077
3. Karami R, Hoseinpour M, Rasul M, et al. (2022) Exergy, energy, and emissions analyses of binary and ternary blends of seed waste biodiesel of tomato, papaya, and apricot in a diesel engine. *Energy Convers Manage* 16: 100288. https://doi.org/10.1016/j.ecmx.2022.100288
4. Mahmood HA, Al-Sulttani AO, Mousa NA, et al. (2022) Impact of lambda value on combustion characteristics and emissions of syngas-diesel dual-fuel engine. *Int J Technol* 13: 179–189. https://doi.org/10.14716/ijtech.v13i1.5060
5. Mohammed WT, Jabbar MFA (2016) Zirconium sulfate as catalyst for biodiesel production by using reactive distillation. *J Eng* 22: 68–82. https://doi.org/10.31026/j.eng.2016.01.05
6. Mahmood HA, Attia OH, Al-Sulttani AO, et al. (2023) Impacts of varied injection timing on emission levels, combustion efficiency, and performance of biodiesel engines. *Math Modell Eng Probl* 10: 1873–1883. https://doi.org/10.18280/mmep.100541
7. Dixit S, Kumar A, Kumar S, et al. (2020) CFD analysis of biodiesel blends and combustion using Ansys Fluent. *Mater Today: Proc* 26: 665–670. https://doi.org/10.1016/j.matpr.2019.12.362
8. Salman SM, Mohammed MM, Mohammed FL (2016) Production of methyl ester (Biodiesel) from used cooking oils via trans-esterification process. *J Eng* 22: 74–88. https://doi.org/10.31026/j.eng.2016.05.06
9. Hussien M (2019) Biodiesel production from used vegetable oil (sunflower cooking oil) using eggshell as bio catalyst. *Iraqi J Chem Pet Eng* 20: 21–25. https://doi.org/10.31699/IJCPE.2019.4.4
10. Beyene D, Bekele D, Abera B (2024). Biodiesel from blended microalgae and waste cooking oils: Optimization, characterization, and fuel quality studies. *AIMS Energy* 12: 408–438. https://doi.org/10.3934/energy.2024019

11. Temizer İ, Cihan Ö, Eskici B (2020) Numerical and experimental investigation of the effect of biodiesel/diesel fuel on combustion characteristics in CI engine. *Fuel* 270: 117523. https://doi.org/10.1016/j.fuel.2020.117523
12. Talupula NMB, Rao PS, Kumar BSP, et al. (2017) Alternative fuels for internal combustion engines: Overview of current research. *SSRG Int J Mech Eng* 4: 17–26. https://doi.org/10.14445/23488360/IJME-V4I4P105
13. Lv J, Wang S, Meng B (2022) The effects of nano-additives added to diesel-biodiesel fuel blends on combustion and emission characteristics of diesel engine: A review. *Energies* 15: 1032. https://doi.org/10.3390/en15031032
14. Renish RR, Selvam AJ, Čep R, et al. (2022) Influence of varying compression ratio of a compression ignition engine fueled with B20 blends of sea mango biodiesel. *Processes* 10: 1423. https://doi.org/10.3390/pr10071423
15. Ahamad Shaik A, Rami Reddy S, Dhana Raju V, et al. (2022) Combined influence of compression ratio and EGR on diverse characteristics of a research diesel engine fueled with waste mango seed biodiesel blend. *Energy Sources, Part A: Recovery, Util, Environ Eff*, 1–24. https://doi.org/10.1080/15567036.2020.1811809
16. Datta A, Mandal BK (2017) An experimental investigation on the performance, combustion and emission characteristics of a variable compression ratio diesel engine using diesel and palm stearin methyl ester. *Clean Technol Environ Policy* 19: 1297–1312. https://doi.org/10.1007/s10098-016-1328-3
17. Rosha P, Mohapatra SK, Mahla SK, et al. (2019) Effect of compression ratio on combustion, performance, and emission characteristics of compression ignition engine fueled with palm (B20) biodiesel blend. *Energy* 178: 676–684. https://doi.org/10.1016/j.energy.2019.04.185
18. Sivaramakrishnan K (2018) Investigation on performance and emission characteristics of a variable compression multi fuel engine fuelled with Karanja biodiesel-diesel blend. *Egypt J Pet* 27: 177–186. https://doi.org/10.1016/j.ejpe.2017.03.001
19. Dugala NS, Goindi GS, Sharma A (2021) Experimental investigations on the performance and emissions characteristics of dual biodiesel blends on a varying compression ratio diesel engine. *SN Appl Sci* 3: 622. https://doi.org/10.1007/s42452-021-04618-0
20. Mahmood AS, Qatta HI, Al-Nuzal SM, et al. (2021) The effect of compression ratio on the performance and emission characteristics of CI Engine fuelled with corn oil biodiesel blended with diesel fuel. *IOP Conference Series: Earth and Environmental Science: IOP Publishing* 779: 012062. https://doi.org/10.1088/1755-1315/779/1/012062
21. Ng HK, Gan S, Ng J-H, et al. (2013) Simulation of biodiesel combustion in a light-duty diesel engine using integrated compact biodiesel-diesel reaction mechanism. *Appl Energy* 102: 1275–1287. https://doi.org/10.1016/j.apenergy.2012.06.059
22. Atgur V, Manavendra G, Desai GP, et al. (2022) CFD combustion simulations and experiments on the blended biodiesel two-phase engine flows. *Appl Comput Fluid Dyn Simul Model: IntechOpen*. https://doi.org/10.5772/intechopen.102088
23. Rajeesh S, Methre J, Godiganur S (2021) CFD analysis of combustion characteristics of CI engine run on biodiesel under various compression ratios. *Mater Today: Proc* 47: 5823–5829. https://doi.org/10.1016/j.matpr.2021.04.193
24. Raza A, Mehboob H, Miran S, et al. (2020) Investigation on the characteristics of biodiesel droplets in the engine cylinder. *Energies* 13: 3637. https://doi.org/10.3390/en13143637

25. Alrazen HA, Aminossadati SM, Mahmood HA, et al. (2023) Theoretical investigation of combustion and emissions of CI engines fueled by various blends of depolymerized low-density polythene and diesel with co-solvent additives. *Energy* 282: 128754. https://doi.org/10.1016/j.energy.2023.128754
26. Belal TM, El Sayed MM, Osman MM (2013) Investigating diesel engine performance and emissions using CFD. *Energy Power Eng* 5: 171–180. https://doi.org/10.4236/epe.2013.52017
27. Lois AL, Al-Lal A, Canoira L, et al. (2012). PAH occurrence during combustion of biodiesel from various feedstocks. *Chem Eng Trans* 29: 1159–1164. https://doi.org/10.3303/CET1229194
28. Ashkezari AZ, Divsalar K, Malmir R, et al. (2020). Emission and performance analysis of DI diesel engines fueled by biodiesel blends via CFD simulation of spray combustion and different spray breakup models: A numerical study. *J Therm Anal Calorim* 139: 2527–2539. https://doi.org/10.1007/s10973-019-08922-1
29. Karami R, Rasul MG, Khan MM (2020) CFD simulation and a pragmatic analysis of performance and emissions of tomato seed biodiesel blends in a 4-cylinder diesel engine. *Energies* 13: 3688. https://doi.org/10.3390/en13143688
30. Efe Ş, Ceviz MA, Temur H (2018) Comparative engine characteristics of biodiesels from hazelnut, corn, soybean, canola and sunflower oils on DI diesel engine. *Renewable Energy* 119: 142–151. https://doi.org/10.1016/j.renene.2017.12.011
31. Jaikumar S, Bhatti SK, Srinivas, V, et al. (2020) Combustion and vibration characteristics of variable compression ratio direct injection diesel engine fuelled with diesel-biodiesel and alcohol blends. *Eng Rep* 2: 12195. https://doi.org/10.1002/eng2.12195